Journal of Contaminant Hydrology xxx (2015) xxx–xxx

Contents lists available at ScienceDirect

Journal of Contaminant Hydrology

journal homepage: www.elsevier.com/locate/jconhyd

Pressure-controlled injection of guar gum stabilized microscale zerovalent iron for groundwater remediation

M. Luna [a], F. Gastone [a], T. Tosco [a], R. Sethi [a,*], M. Velimirovic [b,e], J. Gemoets [b], R. Muyshondt [b], H. Sapion [c], N. Klaas [d], L. Bastiaens [b]

[a] Dipartimento di Ingegneria dell'Ambiente, del Territorio e delle Infrastrutture—Politecnico di Torino, corso Duca degli Abruzzi 24, 10129 Torino, Italy
[b] VITO, Boeretang 200, 2400 Mol, Belgium
[c] SAPION, Oude Bevelsesteenweg 51, 2560 Nijlen, Belgium
[d] VEGAS, University of Stuttgart, Pfaffenwaldring 61, 70569 Stuttgart, Germany
[e] Department of Environmental Geosciences, University of Wien, Althanstrasse 14, 1090 Wien, Austria

ARTICLE INFO

Article history:
Received 26 September 2014
Received in revised form 15 April 2015
Accepted 19 April 2015
Available online xxxx

Keywords:
Microscale zerovalent iron (mZVI)
Field scale mZVI injection
Guar gum
Low pressure injection
Monitoring setup
Chlorinated aliphatic hydrocarbons

ABSTRACT

The paper reports a pilot injection test of microsized zerovalent iron (mZVI) dispersed in a guar gum shear thinning solution. The test was performed in the framework of the EU research project AQUAREHAB in a site in Belgium contaminated by chlorinated aliphatic hydrocarbons (CAHs). The field application was aimed to overcome those critical aspects which hinder mZVI field injection, mainly due to the colloidal instability of ZVI-based suspensions. The iron slurry properties (iron particles size and concentration, polymeric stabilizer type and concentration, slurry viscosity) were designed in the laboratory based on several tests (reactivity tests towards contaminants, sedimentation tests and rheological measurements). The particles were delivered into the aquifer through an injection well specifically designed for controlled-pressure delivery (approximately 10 bars). The well characteristics and the critical pressure of the aquifer (i.e. the injection pressure above which fracturing occurs) were assessed via two innovative injection step rate tests, one performed with water and the other one with guar gum. Based on laboratory and field preliminary tests, a flow regime at the threshold between permeation and preferential flow was selected for mZVI delivery, as a compromise between the desired homogeneous distribution of the mZVI around the injection point (ensured by permeation flow) and the fast and effective injection of the slurry (guaranteed by high discharge rates and injection pressure, resulting in the generation of preferential flow paths). A monitoring setup was designed and installed for the real-time monitoring of relevant parameters during injection, and for a fast determination of the spatial mZVI distribution after injection via non-invasive magnetic susceptibility measurements.

1. Introduction and background

The use of zerovalent iron in the form of microscale or nanoscale particles (mZVI or nZVI) is a promising and cost-effective approach for groundwater remediation. mZVI and nZVI allow to overcome most of the restrictions associated to the use of millimetric iron fillings in permeable reactive barriers (PRBs), mainly related to the difficulties in the excavation of the trench, to the limited depth of application, and to the treatment of the sole dissolved fraction of the contaminants (Di Molfetta and Sethi, 2006; Moraci and Calabrò, 2010; Tosco et al., 2014b; Zhang, 2003; Zolla et al., 2009).

Despite a broad range of laboratory studies have been devoted in recent years to the assessment of reactivity (Freyria et al., 2011; Hosseini et al., 2011) and transport of iron particles in saturated porous media (Dalla Vecchia et al., 2009b; Freyria

* Corresponding author. Tel.: +39 0110907735; fax: +39 0110907699.
E-mail address: rajandrea.sethi@polito.it (R. Sethi).

http://dx.doi.org/10.1016/j.jconhyd.2015.04.007
0169-7722/

et al., 2011; Hosseini and Tosco, 2013; Tiraferri and Sethi, 2009; Tosco et al., 2014a), successful and well controlled pilot scale studies proving the feasibility of this approach are still limited, and mostly performed using nZVI (Bennett et al., 2010; Elliott and Zhang, 2003; Johnson et al., 2013; Macé et al., 2006; Mueller et al., 2012; O'Carroll et al., 2013; Quinn et al., 2005; Su et al., 2012), while mZVI field injection has been scarcely reported (Flores Orozco et al., 2015; Luna et al., 2013; Truex et al., 2011). The most critical issue in field scale applications of zerovalent iron particles is related to the generation of a wide and homogeneous reactive zone (Cameselle et al., 2013; Cook, 2009; EPA, 2003; Quinn et al., 2005). Several concurrent factors have to be taken into account to achieve optimal results, including (a) stability of the ZVI suspensions, (b) mobility of the ZVI particles, (c) injection approach, and (d) costs.

The emplacement of ZVI particles is hindered by the strong magnetic interactions which lead to aggregation and subsequent gravitational settling of bigger flocs (Dalla Vecchia et al., 2009a; Phenrat et al., 2007; Tiraferri et al., 2008). Such aggregates could also significantly limit transport and clog the porous medium (Kanel et al., 2005; Kocur et al., 2013; Liu et al., 2005; Phenrat et al., 2007; Phenrat et al., 2010; Saleh et al., 2007; Schrick et al., 2004). They also exhibit reduced specific surface area, and therefore reactivity (He and Zhao, 2005; Nurmi et al., 2005). Aggregation and sedimentation of ZVI particles should be prevented for a time sufficient to allow slurry preparation, handling and injection in the subsurface. An improved colloidal stability can be obtained by adding surfactants or food-grade green biopolymers characterized by high molecular weight. Polymers, if dosed in low concentration (fractions of g/l), adsorb on the particle surface, creating a brush layer and thus reducing inter-particle forces (steric stabilization) (Hydutsky et al., 2007; Krol et al., 2013; Phenrat et al., 2008; Schrick et al., 2004; Tiraferri et al., 2008; Tosco and Sethi, 2010). The polymer anchored onto the ZVI particles has a double positive impact on particles mobility: it reduces particle–particle attractive forces, preventing the formation of large aggregates which may be prone to filtration in the porous medium, and at the same time increases the repulsion among particles and porous medium. Since the adsorption of biopolymer chains can hinder the reactivity, it is important to use easily biodegradable biopolymers (e.g. guar gum) which can be removed by enzymatic breakdown (Di Molfetta and Sethi, 2006; Gastone et al., 2014a; Kirschling et al., 2011; Reddy et al., 2011; Velimirovic et al., 2012) or by soil microbial population (Velimirovic et al., 2014b). If the polymer is dosed in significantly higher concentrations (in the order of grams per liter), part of the polymer chains adsorb onto the ZVI surface, until saturation, and part stay in suspension, increasing the viscosity of the dispersing fluid (kinetic stabilization) and consequently significantly reducing aggregation and sedimentation rate (Dalla Vecchia et al., 2009b; Tiraferri et al., 2008; Velimirovic et al., 2012; Xue and Sethi, 2012). Stabilization approaches based on the use of polymeric solutions, characterized by a non-Newtonian shear thinning behavior, showed promising results also in improving particles mobility in porous media (Cantrell et al., 1997; Comba and Sethi, 2009; Dalla Vecchia et al., 2009b; Gastone et al., 2014b; Kocur et al., 2013; Tiraferri and Sethi, 2009; Tiraferri et al., 2008; Tosco et al., 2014a; Xue and Sethi, 2012). In particular, Dalla Vecchia et al. (2009b) and Hydutsky et al. (2007) proved that the transport distances of polymer-coated nZVI and mZVI can be in the order of a meter in laboratory experiments. Furthermore, from a rheological point of view, the shear thinning behavior of guar gum solutions is highly beneficial for field applications, since it helps improving stability without significantly increasing the injection pressure: shear thinning fluids show a viscosity decrease as the shear rate increases, i.e. the viscosity is higher in static conditions (corresponding to the storage before injection) and lower in dynamic conditions (corresponding to the injection in the subsurface, when a limited viscosity is desired in order to limit the overall pressure build-up in the porous medium) (Comba et al., 2011; Sorbie et al., 1989; Xue and Sethi, 2012).

Even if some successful pilot and full scale applications of both nZVI and mZVI have been recently reported using different injection technologies (Elliott and Zhang, 2003; He et al., 2010; Johnson et al., 2013; O'Carroll et al., 2013; Quinn et al., 2005; Su et al., 2012; Velimirovic et al., 2014c), specific studies on the preferable delivery techniques are, to the authors' knowledge, still lacking, and the topic still needs to be further investigated. As a general rule, a field injection can be performed according to two different regimes: (i) permeation injection, which generates a uniform particle distribution in the subsurface and ensures the contact between particles and contaminants, or (ii) fracturing injection, which consists in injecting fluids and particles at a pressure exceeding the porous medium critical pressure, thus generating a non-uniform distribution if the process is not properly designed and controlled. From a theoretical point of view, in order to achieve a homogeneous distribution of the particles around the delivery point, the injection via permeation is preferable to fracturing. Nevertheless, there are several factors that hinder the delivery under permeation regime, namely medium to low hydraulic conductivity of the aquifer system, and mechanical straining of the particles when the ratio of the size of the iron particles to grain size of the aquifer material exceeds a threshold limit, usually reported in the range of 0.8–1% (Bradford et al., 2006; Xu et al., 2006). Moreover, the injection has to be performed in a time shorter than the sedimentation time of the particles, in order to avoid plugging of the injection pipes and of the well. As a consequence, the injection discharge has to be chosen fulfilling two requirements: on the one hand it has to be low enough to avoid pressure build-up exceeding the porous medium critical value, on the other hand it has to be high enough to ensure colloidal stability during the whole injection. Finally, it is worth to point out that adopting very low discharge rates, and consequently increasing the overall delivery time, leads to a significant increase in costs due to longer field injection operations. Similar considerations are also valid for the determination of the stabilizer concentration: on the one hand it should be high enough to maintain the particles suspended for the duration of the injection, on the other hand it should be low enough to prevent excessive pressure build-up in the well.

As highlighted in this paragraph, the design of a field scale injection of ZVI-based slurries is the result of the optimization of several concurrent technical, environmental and economic factors and constraints which have to be simultaneously satisfied. In several field applications a permeation injection is practically unfeasible, due to the constraints mentioned above, and fracturing injection is the only viable approach. As an example, the authors previously reported a field injection in a low permeability contaminated aquifer, where the ratio of

Please cite this article as: Luna, M., et al., Pressure-controlled injection of guar gum stabilized microscale zerovalent iron for groundwater remediation, J. Contam. Hydrol. (2015), http://dx.doi.org/10.1016/j.jconhyd.2015.04.007

particle to aquifer grain size greatly exceeded the threshold limit for straining (Velimirovic et al., 2014c). In that study, the low permeability of the medium, the use of large mZVI particles (in the order of several tens of microns), and consequently the need of a high polymer concentration (7.2 g/l, resulting in a zero shear viscosity close to 10 Pa s), required a high injection pressure, and a direct push delivery system was adopted. On the contrary, in the present study, the application to a fairy permeable aquifer is described, and the general criteria for the design, realization and monitoring of a pilot-scale permeation injection of mZVI particles are discussed. Injection via a screened pressurized well was preferred to other delivery techniques to guarantee a higher control of the delivery pressure. The design was conducted taking into account all critical aspects previously discussed, focusing on the optimization of both injection and monitoring strategy. The injection was performed in a flow regime on the threshold between permeation and fracturing aiming to generate a large and likely homogenous reactive zone. From a technical point of view, innovative solutions were adopted for (i) the design of an injection well suitable for pressure injection at moderate flow rate preventing product daylighting, (ii) the determination of the critical fracturing pressure from a step rate injection test, (iii) an improved preparation method of the suspensions to avoid the presence of polymer flocs and particle aggregates, and finally (iv) an innovative and efficient monitoring setup for the real-time control of the relevant parameters during injection and for the spatial reconstruction of the final mZVI distribution in the subsurface.

2. Experimental section

2.1. Site description

The site selected for the pilot test injection, herein denominated Site P, is an active industrial site located in Belgium, contaminated by chlorinated aliphatic hydrocarbons (CAHs). For the pilot injection described below a test area of approximately 100 m × 80 m in the parking area outside the plant was selected on the basis of contaminants characterization data (Fig. 1). From a hydrogeological point of view, the site is characterized by fine sand with several local heterogeneities; the subsoil average bulk density is 1850 kg/m^3 and the effective porosity was estimated equal to 0.2. The grain size distribution (GSD) along the depth was determined from samples collected during the drilling of the injection well (Table 1). The average depth to water table is 2 m, the hydraulic gradient is 0.07% and the groundwater effective velocity is 5×10^{-3} m/day. The average hydraulic conductivity was determined by slug test equal to 1.8×10^{-5} m/s. The values along the depth were estimated applying Hazen's formula $K = 100 \cdot d_{10}^2$ (units in cm/s and cm, respectively) (Gastone et al., 2014a; Hazen, 1892; Hazen, 1911) and are reported in Table 1.

Since the contaminant source is assumed to be located below a building, it was not possible to undertake a detailed characterization for the source of contamination (Fig. S5 in Supporting Information). However, the most contaminated spot in the plume is located approximately 20 m SW from the injection well with a maximum concentration of tetrachloroethene (PCE) equal to 73 mg/l (Fig. S5 in Supporting Information). Concentrations of PCE equal to 3.5 mg/l, trichloroethene (TCE) equal to 0.7 mg/l and *cis*-dichloroethene (cDCE) equal to 0.5 mg/l were measured in the groundwater samples extracted 2 weeks before injection from the injection well (4.5 to 7 m-bgl).

2.2. Iron particles and biopolymer

In this study microscale iron particles were preferred over nanoscale ones due to their significantly lower cost, in the order of 6 to 30 €/kg, compared to approximately 100 €/kg for the nanoscale particles. Several commercially available mZVI particle brands were considered and most of them proved to be able to effectively degrade the afore mentioned chlorinated hydrocarbons under batch conditions, but the finest sample (Carbonyl Iron Powder HQ, BASF, Germany), was chosen in order to reduce particle filtration during the injection. HQ particles are characterized by a fine granulation (d_{10}, d_{50}, d_{90} equal to 0.84, 1.40, 2.29 μm respectively, measured by laser

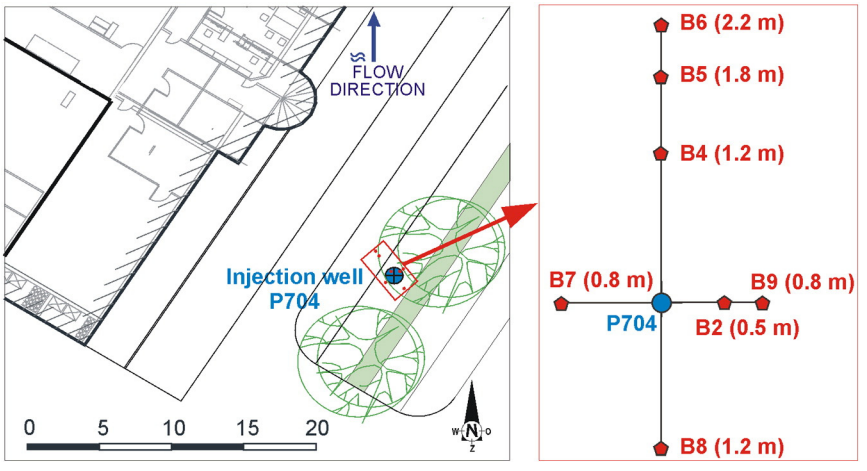

Fig. 1. Map of the test area and liner position around the injection well P704.

Please cite this article as: Luna, M., et al., Pressure-controlled injection of guar gum stabilized microscale zerovalent iron for groundwater remediation, J. Contam. Hydrol. (2015), http://dx.doi.org/10.1016/j.jconhyd.2015.04.007

Table 1
Variation along the depth of grain size distribution of the aquifer material, hydraulic conductivity and ratio of mZVI average diameter (d_{50} = 1.40 μm) to d_{10} of the aquifer material. The hydraulic conductivity was estimated using Hazen's formula $K = 100 \cdot d_{10}^2$ (units in cm/s and cm, respectively).

Depth (m-bgl)	d_{10} (μm)	d_{50} (μm)	d_{90} (μm)	K (m/s)	$d_{50,mZVI}/d_{10,sand}$ (%)
2–3	125	231	468	1.6×10^{-4}	1.1
3–4	129	227	428	1.7×10^{-4}	1.1
4–5	101	227	449	1.0×10^{-4}	1.4
5–6	24	112	251	5.8×10^{-6}	5.8
6–7	28	238	1062	7.9×10^{-6}	5.0

diffraction using a Mastersizer 2000, Malvern, UK), spherical shape, very high purity (iron content in the range of 97–98%) and large specific surface area (Schlicker et al., 2000; Su and Puls, 2004; Velimirovic et al., 2013; Westerhoff, 2003). Nevertheless, HQ particles, if dispersed in pure water, are very unstable and prone to partial aggregation and fast sedimentation, due to their micrometric size, high density (close to bulk iron density of 7.8 g/cm^3), and weak attractive forces among particles. The colloidal stability was therefore improved by means of a food-grade guar gum (HV700, RANTEC, United States) characterized by high molecular weight and fast degradation rate in the presence of enzymes (Di Molfetta and Sethi, 2006; Gastone et al., 2014a; Tiraferri and Sethi, 2009; Velimirovic et al., 2012). HV700 is provided as dry powder with a medium to fine granulation (nominal maximum grain size equal to 75 μm), which can be easily dissolved in water increasing fluid viscosity and forming a shear thinning solution (Comba and Sethi, 2009; Gastone et al., 2014a; Gastone et al., 2014b; Wang et al., 2008).

Despite the small granulation of the HQ powder, a partial retention of the particles is expected to occur due to straining or wedging (Raychoudhury et al., 2014), since the ratio of the average particle size d_{50} to the d_{10} of the aquifer material (Table 1) is close to or higher than the straining limit of 0.8–1% (Xu et al., 2006).

2.3. Laboratory sedimentation and rheological tests

Laboratory studies were conducted in order to determine the optimal polymer concentration able to stabilize the selected mZVI particles during the injection for the desired time, and to define the most cost- and time-effective preparation method. In this study, the proper concentration of mZVI particles in the slurry was identified to be equal to 10 g/l. This value was defined as a function of the target concentration to be reached in the subsoil after the field injection, basing on reactivity tests (Supporting Information), and design parameters (i.e. injected volume and radius of influence), which will be defined in the following paragraphs.

The efficacy of the slurry preparation procedure was evaluated based on sedimentation and rheological experimental results for samples prepared with three different dissolution methods, namely: (i) mechanical mixing at room temperature, (ii) mechanical mixing with water heated up to 60 °C and (iii) dissolution at room temperature using a high speed rotor-stator system (Ultra Turrax).

Guar gum solution was continuously stirred until completed dissolution of the powder, and used immediately after preparation. Air bubbles were removed by degassing the solution using a vacuum pump.

To prepare the mZVI slurry, mZVI particles were added into the polymer solution while stirring and later on the suspension was mixed several minutes at high speed using a rotor-stator system (UltraTurrax UTL-25, IKA, Germany) to break mZVI aggregates and to homogeneously disperse the particles. The slurry was degassed under vacuum prior to use.

The flow behavior of the suspensions was assessed through rheological tests using a rheometer (MCR 301, Anton Paar, Austria) equipped with coaxial cylinders, measuring viscosity in a shear rate range corresponding to the interval relevant for the field radial injection (Sorbie et al., 1989; Tosco et al., 2014a), namely from 10^{-2} to 10^3 s^{-1}.

Sedimentation tests of HQ slurries (10 g/l of iron particles, 2 g/l of guar gum in deionized water) were conducted by monitoring the evolution of iron concentration over time using a susceptibility sensor (Bartington, UK). The sedimentation half-time (t_{50}) was determined as the time when the measured susceptibility (directly proportional to the mZVI concentration) matches half its initial value (Dalla Vecchia et al., 2009b; Gastone et al., 2014a).

2.4. Injection well and pumping system

An injection well (P704) was specifically designed for the pilot test in order to sustain average to high discharge rates. The well was properly sealed on top to avoid product daylighting. Completion data and a schematic graphic representation are reported in Fig. 2. The well is characterized by a PVC pipe with an internal diameter of 100 mm and a screen length L_s of 2.5 m (from 4.5 to 7 m-bgl). The annular space between the well screen (slot size of 0.5 mm) and the 219 mm borehole (D_d) was filled with a filter pack with an average grain size of 2.5 mm. The size of the filter slot and of the filter gravel was selected large enough to limit head losses and pressure build-up during the slurry injection. Aiming to improve the sealing, a larger drilling diameter ($D_{sealing}$) equal to 500 mm was adopted above the filter pack, and the annular space between the blind tubing and the borehole was filled with cement. Furthermore, a 30 cm thick layer of swelling bentonite pellets was placed between the drain and the cement. Finally, the top of the well was closed by a plug cap able to provide the sealing required to pressurize the well during the injection.

The fluids were injected using a lobe pump (24-A1, Jabsco, Germany), specifically designed for the injection of highly viscous fluids, able to sustain high injection pressure (up to 15 bars) and to provide an almost constant discharge rate (up to 95 l/min).

2.5. Field preparation of guar gum and mZVI slurries

Guar gum slurries were prepared by means of a powder dispersing unit used in food industry (YTRON-ZC ViscoTron, YTRON, Germany), which allows to achieve high hydration and viscosity very quickly (Fig. 3). The guar gum powder was dosed in the funnel and then mixed into the dispersing unit with water flowing from the 200 l tank. The solution was then recirculated for few minutes while stirred inside the main tank by means of a rotating head. Once hydrated, the guar gum

Please cite this article as: Luna, M., et al., Pressure-controlled injection of guar gum stabilized microscale zerovalent iron for groundwater remediation, J. Contam. Hydrol. (2015), http://dx.doi.org/10.1016/j.jconhyd.2015.04.007

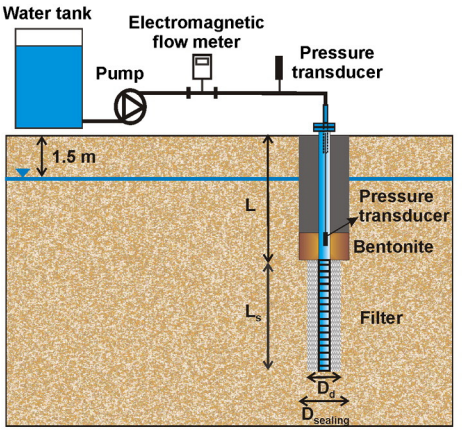

Injection well (P704)	
Tubing diameter (mm)	110
Material	PVC-HDPE
Total length (m)	7
Length of the screen Ls (m)	2.5
Sealing length L (m)	4.5
Drain diameter D_d (mm)	219
Sealing diameter $D_{sealing}$ (mm)	324
Top diameter D_{top} (mm)	500
Gravel pack grain size (mm)	2 - 3
Slot size of the tubing (mm)	0.5

(b)

Fig. 2. Water injection step rate setup and well characteristics.

solution was transferred in a 1 m^3 vessel, continuously fed from the disperser, and connected to the injection circuit.

The mZVI slurry was prepared in a conic mixing vessel of 1 m^3 capacity, provided with a rotating head and a recirculation system, and connected to a high speed rotor-stator based dispersing unit (DK40, CAT, Germany) able to break aggregates and obtain well dispersed and stable suspensions. Iron particles were placed in the conic vessel filled with guar gum solution, mixed and recirculated (Fig. 3).

2.6. Water and guar gum injection step rate test

Two step rate tests were performed on the new injection well, injecting water in the first test, and guar gum in the second one. Contrary to traditional step rate tests, which usually involve the extraction of water with a stepwise increase of discharge rate, in this application the two tests were conducted injecting the fluid, coherently with the envisioned use of the well. The tests were aimed at assessing the hydraulic efficiency of the injection well and its behavior after the overcoming of the critical fracturing pressure.

The first test consisted in injecting water at constant, stepwise-increased discharge rate. Each step lasted for 2 h, respectively injecting at 0.6, 1.2, 1.7 and 2.15 m^3/h. The second test was aimed at assessing the injectability of the non-Newtonian guar gum solution and at evaluating the pressure build-up which can be generated during the pilot test. It consisted in three injection steps (discharge rate respectively equal to 0.5, 1 and 1.5 m^3/h) of 2 g/l guar gum solution.

During both tests, the fluid level in the injection well, the injection pressure and the discharge rate at well were continuously monitored. After the guar gum injection test, the well was flushed for 2 h with water at high discharge rate (2.2 m^3/h) in order to remove guar gum residuals before the subsequent mZVI injection.

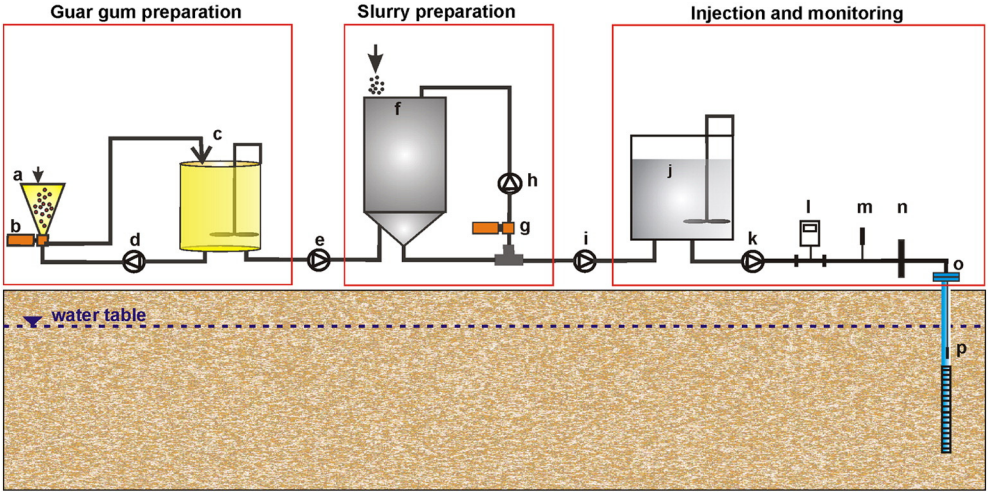

Fig. 3. Slurry preparation, injection and monitoring system. a) Funnel for guar gum powder; b) dispersing unit; c) cylindrical vessel with mixing system; d) piston pump for recirculation; e) pump; f) conic vessel for mZVI slurry preparation; g) mZVI dispersing unit; h-i) screw pumps; j) mZVI slurry cubic container; k) lobe pump for injection; l) electromagnetic flowmeter; m) pressure transducer; n) magnetic susceptibility sensor; o) well plugging system; and p) pressure transducer.

Please cite this article as: Luna, M., et al., Pressure-controlled injection of guar gum stabilized microscale zerovalent iron for groundwater remediation, J. Contam. Hydrol. (2015), http://dx.doi.org/10.1016/j.jconhyd.2015.04.007

2.7. Monitoring setup

In order to monitor the injection process (injection pressure, injection discharge and volume) and the properties of the injected fluids (viscosity and mZVI concentration), a specific monitoring setup was adopted. The discharge rate and total injected volume were continuously measured in-line using an electromagnetic flowmeter (Promag 30, Endress + Hauser, Switzerland). The pressure was recorded by two pressure transducers, the first in the injection well (Levelogger M100, Solinst, Canada), the second (HD2124.1, Delta Ohm, Italy) connected to the injection pipe to monitor real-time injection pressure. The preparation, injection and monitoring setup are shown in Fig. 3.

The viscosity of the injected slurry was assessed from collected samples through a Marsh Funnel, commonly used for quick evaluation under field condition of rheological properties of drilling fluids. The mZVI concentration during injection was determined via in-line non-invasive monitoring of magnetic susceptibility. For this purpose, a magnetic susceptibility meter coupled with a core logging sensor (MS2 and MS2C, Bartington, UK) was used. The sensor consists of an AC wound inductor to which a low intensity oscillating magnetic field is applied. The sensor is suitable for measurements on cores and cylindrical samples, which are placed coaxially to it, within the inductor. Frequency perturbations are induced by the presence of the sample, and the signal is processed to retrieve its magnetic permeability, directly related to the magnetic susceptibility. Since for a dispersion of ferromagnetic particle the susceptibility value is linearly proportional to the mass of particles (Dalla Vecchia et al., 2009a; Dalla Vecchia et al., 2009b), the mZVI concentration can be directly obtained from susceptibility measurements. During slurry injection, the sensor was placed coaxially to the inlet tubing, providing the evolution over time of injected slurries mZVI concentration.

To assess the final mZVI distribution in the subsurface, after the mZVI injection test 9 core samples were collected around the injection well at different radial distances (Fig. 1). The liners were retrieved using a Geoprobe system at depths ranging between 2.4 and 7 m-bgl. Since the aquifer is characterized by

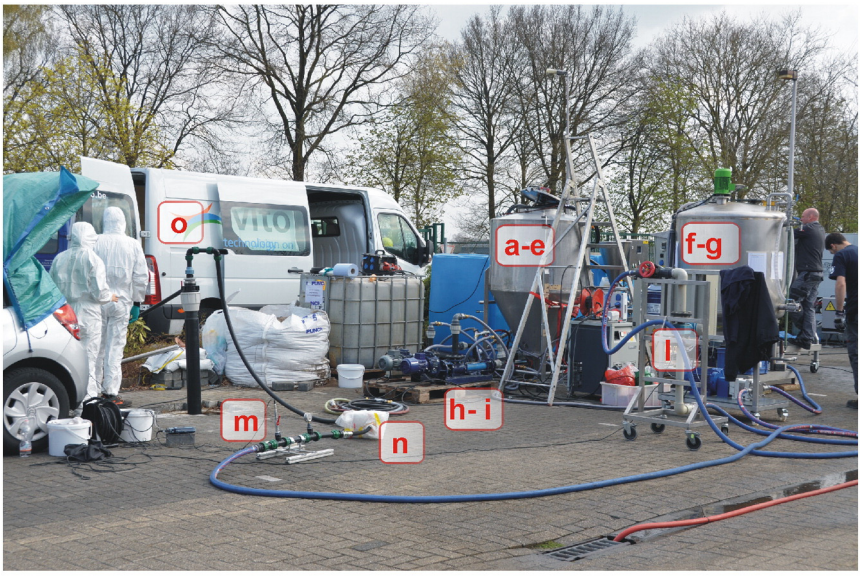

(a)

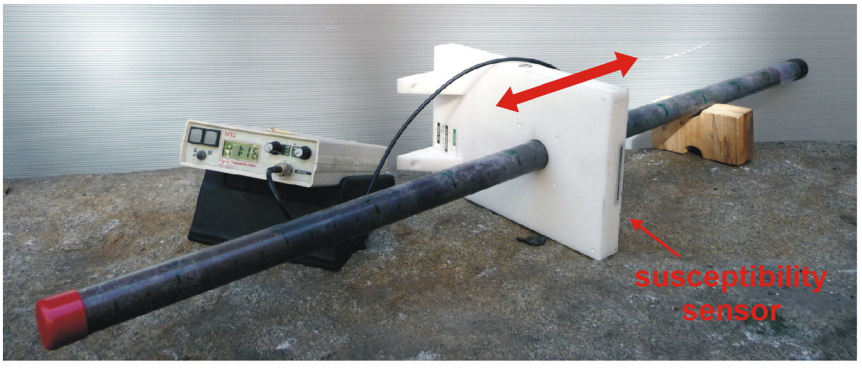

(b)

Fig. 4. (a) Pilot test equipment (refer to caption of Fig. 3 for labeling), and (b) measurement of susceptibility along the cores using MS2C sensor.

Please cite this article as: Luna, M., et al., Pressure-controlled injection of guar gum stabilized microscale zerovalent iron for groundwater remediation, J. Contam. Hydrol. (2015), http://dx.doi.org/10.1016/j.jconhyd.2015.04.007

fine solid matrix, the sample recovery, i.e. the ratio of the length of recovered sample to the length of sampler advancement (USEPA, 1998), was about 95%. The magnetic susceptibility was measured directly in the field, using the susceptibility sensor already employed for the in-line monitoring of the mZVI injected concentration. The sensor was positioned coaxially to the core, and moved along it (Fig. 4). The susceptibility values were recorded each 10 cm, which is a measuring distance long enough to ensure no correlation between consecutive values (Dalla Vecchia et al., 2009b; Tosco et al., 2014a). A detailed description of the method is provided in the Supporting Information. The concentration of zerovalent iron was determined via hydrogen (H_2) gas evolution after acid digestion (Velimirovic et al., 2014b) of a limited number of samples taken from the cores at depths and directions of particular interest (zero-, mean-, maximum-iron concentration) and used for the calibration of susceptibility to concentration values (Supporting Information).

2.8. Groundwater sampling

To monitor the concentration of CAHs over time in the well, groundwater samples were collected after the injection by connecting the PTFE tubing placed in the well with a peristaltic pump (Eijkelkamp, The Netherlands) at various time intervals (14 days before and 1, 12, 29, 57, 82, 132 and 162 days after the mZVI injection). Field parameters were measured in a flow-through cell by a portable multi-paramater probe (Multi 340i, WTW, Germany) equipped with pH, temperature electrode (SenTix41, WTW, Germany), conductivity measuring cell (TetraCon 325, Global Water, USA), and Liq-Glass redox potential (ORP) electrode (Hamilton, USA). 20 ml of groundwater samples were collected for CAHs analysis in 37 ml vials capped with butyl/PFTE grey septa. The concentrations of CAHs, intermediate- and end-products were obtained the same day via direct head-space measurements using a Varian GC-FID (Velimirovic et al., 2013). Moreover the concentration of guar gum was quantified by phenol-sulfuric acid test using a colorimetric method (DuBois et al., 1956).

3. Results and discussion

3.1. Laboratory sedimentation and rheological tests: dissolution method

Three fast, easy to be up-scaled dissolution methods were evaluated in laboratory tests to identify the procedure which reduces the preparation time and provides a good dissolution of the guar gum powder. A good dissolution is fundamental to minimize the guar gum concentration required to achieve the desired viscosity and to reduce the presence of undissolved particles, which can contribute to the clogging of the porous medium during injection (Gastone et al., 2014b). Experimental data indicate that the best results in terms of stability and solubility are obtained when dissolving polymer powder at room temperature using a high-speed rotor-stator or alternatively dissolving the guar gum at 60 °C. The use of a good dispersion system guarantees the fastest hydration rate, an increased dissolution and, consequently, a sharp reduction of undissolved particles.

The optimal guar gum concentration was determined by means of sedimentation and rheological experiments as the minimum concentration which can guarantee the colloidal stability of the slurry for the entire duration of the injection. The viscosity curves and sedimentation test results obtained for the three guar gum concentrations and the selected preparation method are reported in Fig. 5. A minimum target stability time of 3 h was considered, corresponding to the total time required for the field injection of the mZVI slurry. For guar gum concentrations of 1.5, 2 and 3 g/l, sedimentation half times of, respectively, 1.4, 3.8 and 11.6 h were obtained (Fig. 5a). For the field application, 2 g/l was selected as the optimal guar gum concentration, since 1.5 g/l would not guarantee a sufficient colloidal stability. Moreover, 2 g/l was preferred to 3 g/l since

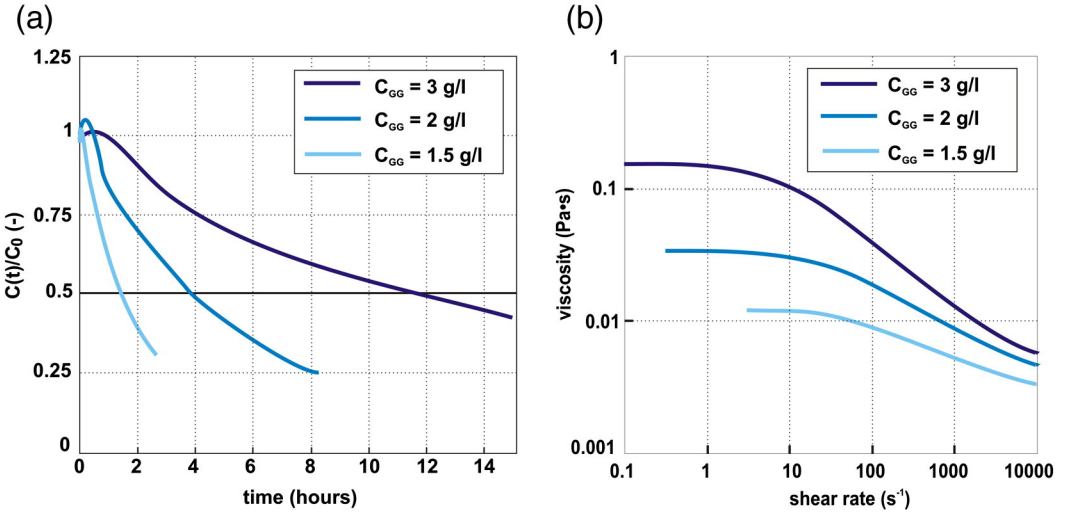

Fig. 5. (a) Sedimentation curves and (b) rheograms of HQ particles (10 g/l) dispersed in guar gum solution (1.5 g/l, 2 g/l, 3 g/l) prepared dissolving polymer at room temperature using a high shear mixer (Ultra-Turrax). In (a) the curves are expressed as normalized concentration C/C_0; the black line refers to the reference ratio $C(t) / C_0 = 0.5$.

Please cite this article as: Luna, M., et al., Pressure-controlled injection of guar gum stabilized microscale zerovalent iron for groundwater remediation, J. Contam. Hydrol. (2015), http://dx.doi.org/10.1016/j.jconhyd.2015.04.007

the latter has a significantly higher viscosity (almost one order of magnitude at low shear rates compared to 2 g/l), and consequently would result in much higher injection pressure (see Fig. 5b), thus leading to fracturing of the porous matrix and preferential flow.

3.2. Water injection step rate test

The first preliminary injection test was aimed at hydraulically characterizing the performance of the injection well in a wide range of discharge rate (from 0.6 to 2.15 m^3/h) and at determining the relationship between injection flow rate and measured pressure build-up.

Before the test, the formation critical pressure was estimated by applying the cavity expansion theory presented by Mitchell and Soga (2005), to verify that injection was in the permeation regime for all steps. The critical injection pressure, which is the maximum injection pressure that can be achieved before the generation of fracture and consequently preferential flow, was estimated in drained conditions. Under the assumption of steady-state radial flow from a cylindrical cavity and elastic behavior of the soil, horizontal cracks can develop by injecting fluids at a pressure that exceeds the total vertical stress in initial conditions (Mitchell and Soga, 2005):

$$P_f = u_0 + \sigma'_{vi} \quad (1)$$

where u_0 is the initial pore pressure (kPa) and σ_{vi}' is the initial vertical effective stress (kPa). The critical pressure at a depth of 5.75 m (which corresponds to the middle point of the screened depth), considering a soil bulk density equal to 1850 kg/m^3, was determined equal to 104 kPa (which correspond to 10.4 mH_2O).

The pressure build-up was continuously monitored during the injection to check whether the estimated threshold value was overcome. Fig. 6a shows the field test results of the water injection step rate test. The pressure is reported as equivalent water level (mH_2O) for a straightforward comparison of the graphs with those typical of step drawdown tests. It can be observed that even at the maximum discharge rate (2.15 m^3/h), the pressure in the well is approximately 5 mH_2O, a value slightly lower than half the critical value estimated from Eq. 1.

The test results were interpreted in the same way as a step drawdown test in order to determine the well characteristic curve, following the Rorabaugh method (Di Molfetta and Sethi, 2012; Rorabaugh, 1953): the overpressure at the end of each injection step, expressed as equivalent increase in water level (s_m), normalized to the corresponding discharge rate (s_m/Q), was reported as a function of the discharge rate, and least-squares fitted to the Jacob's equation (Rorabaugh, 1953; Sethi, 2011):

$$s_m = BQ + CQ^2 \quad 2$$

where s_m is assumed positive for a level increase and Q is assumed positive for injection (i.e. the opposite of step drawdown tests). The linear interpolation of s_m/Q vs Q (Fig. 7) allowed to determine B and C, equal respectively to 2.88×10^6 s/m^2 and 6552 s^2/m^5. The test proved that the well is able to sustain quite high water discharge rate without increasing the pressure above the critical threshold value.

3.3. Guar gum injection step rate test

A further injection step rate test using guar gum was performed prior to inject the mZVI slurry. The guar gum

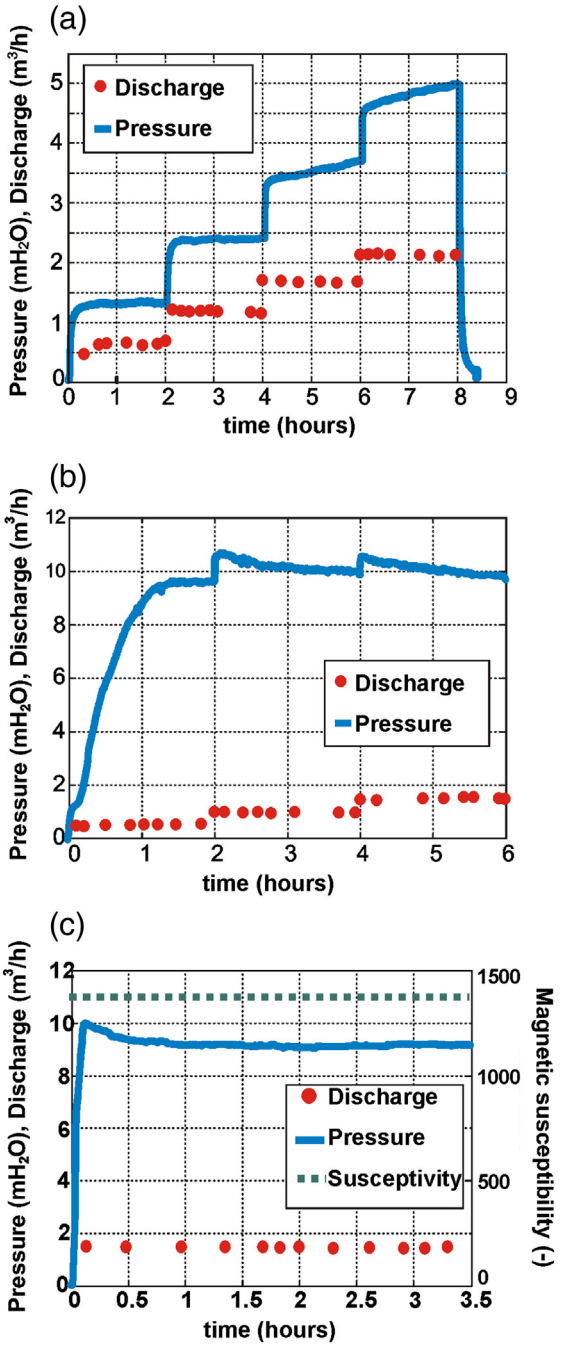

Fig. 6. Pressure and discharge rate monitoring in P704 during (a) water injection step rate test, (b) guar gum injection step rate test, and (c) mZVI pilot injection.

Please cite this article as: Luna, M., et al., Pressure-controlled injection of guar gum stabilized microscale zerovalent iron for groundwater remediation, J. Contam. Hydrol. (2015), http://dx.doi.org/10.1016/j.jconhyd.2015.04.007

injection test was required due to the non-Newtonian properties of the guar gum solutions, which make unfeasible the direct application of the Jacob's equation obtained from the water test for the estimate of the pressure build-up during mZVI slurry injection.

Discharge rates slightly lower than those of the previous test (0.5, 1 and 1.5 m^3/h) were adopted since, due to the higher viscosity of the injected fluid, a higher pressure build-up was expected. The maximum pressure reached at each step (9.65, 10.62 and 10.63 mH_2O) is significantly higher compared to those of water injection (Fig. 6b). A remarkably different trend can be observed in the second and third steps, in which the injection pressure increases until a peak value and then slightly decreases, reaching an asymptotic lower value. This behavior can be explained with a partial generation of preferential flow paths, and this hypothesis is coherent with the peak pressure reached in both steps (10.62 and 10.63 mH_2O, respectively), which is slightly higher that the estimated critical pressure (10.4 mH_2O). On the other hand the steady state pressure value is slightly lower than the critical one (10.03 and 9.80 mH_2O, respectively for the second and third step).

Due to the non-Newtonian behavior of the injected fluids and to the generation of preferential flow paths, it was impossible to determine an accurate and reliable relationship between injection discharge rate and pressure. Nevertheless, the test is useful to foresee the pressure build-up and to select the adequate discharge rate for the pilot injection. Moreover, the test allowed to prove the effectiveness of the guar gum preparation system and to test it before the mZVI slurry injection.

3.4. mZVI slurry preparation, field injection and monitoring

The designed setup for the mZVI slurry preparation allowed to easily disperse the iron particles in the guar gum suspension and, thanks to the coupled dispersion and recirculation system, 1 m^3 of mZVI slurry per hour was prepared.

The pilot mZVI injection test was dimensioned on the basis of the results of laboratory and field preliminary tests. The volume of slurry to be injected in the pilot test was estimated on the basis of the expected radius of influence of the slurry

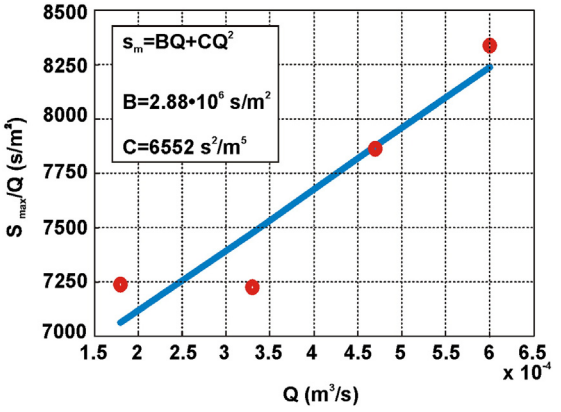

Fig. 7. Analysis of the monitoring results during water injection test: normalized level variation (s_m/Q) as a function of the discharge rate Q for each step (point values) and interpolation using Rorabaugh's equation.

(ROI_s) and on the geometry of the injection well. As a general rule, the volume of aquifer pores (PV) for a given radial distance R from the injection well can be determined by:

$$PV = n_e \cdot \pi \cdot R^2 \cdot L_s \quad (3)$$

where n_e is the effective porosity (here assumed equal to 0.2 based on the site characterization) and L_s (m) is the well screen length (here equal to 2.5 m). A ROI_s of 1 m was defined as target travel distance for this application and a correspondent pore volume equal to 1.57 m^3 was obtained. However, the volume of slurry to be injected in order to guarantee the defined ROI_s at the target concentration is significantly higher than the PV, due to the interactions between iron particles and solid matrix (Elimelech and O'Melia, 1990; Krol et al., 2013). Preliminary mZVI transport simulations performed in a radial domain with porous medium properties similar to those of the test site, under different injection scenarios (different discharge rates, injected volumes and injection times) were performed using MNMs (Tosco et al., 2014a). The simulation results indicated that the volume to be injected for reaching $ROI_s = 1$ m is approximately three times the corresponding pore volume. As a consequence, a safety factor of 3 was applied, and 5 m^3 of mZVI slurry were injected (Table 2). The slurry was prepared in 5 batches of 1 m^3 each and sequentially injected without stopping the pump.

The discharge rate was defined as a compromise between the necessity of avoiding sedimentation of the iron particles and achieving a likely uniform distribution without excessive accumulation close to the injection well. Even if preliminary tests proved that discharge rates higher than 1 m^3/h generate pressure build-up close to or higher than the threshold for preferential flow, it was necessary to select higher values to avoid particle sedimentation and the use of higher polymer concentrations (aiming not to increase fluid viscosity). Therefore, the injection discharge of 1.5 m^3/h was selected for the pilot injection in order to inject 5 m^3 of mZVI slurry in a time almost equal to the sedimentation time of the slurry (t_{50} ~ 4 h).

In Fig. 6c the measured pressure and the injection discharge rate of the mZVI slurry over time are reported. As expected, the injection pressure shows the same trend of the second and third discharge steps of guar gum injection, proving that injection occurred at the threshold between permeation and preferential flow regimes. Moreover, since the injection pressure is of the same order of magnitude as the guar gum injection (the peak value is 9.9 mH_2O and the asymptotic value 9.1 mH_2O), the presence of the iron

Table 2
Properties of the mZVI slurry injected in the pilot test.

Parameter		Value
HQ particle size distribution	d_{10} (μm)	0.84
	d_{50} (μm)	1.40
	d_{90} (μm)	2.29
Slurry properties	mZVI concentration (g/l)	10
	Guar gum concentration (g/l)	2
	Volume injected (m^3)	5
	Discharge rate (m^3/h)	1.5
Sedimentation half-time t_{50} (h)		3.34
Zero shear viscosity μ_0 (Pa s)		0.033

Please cite this article as: Luna, M., et al., Pressure-controlled injection of guar gum stabilized microscale zerovalent iron for groundwater remediation, J. Contam. Hydrol. (2015), http://dx.doi.org/10.1016/j.jconhyd.2015.04.007

particles demonstrated not to significantly influence the initial value of this parameter, nor its evolution over time. This finding suggests that iron particles did not cause a significant clogging of the porous medium, since no increase over time was observed in the pressure data.

The evolution of magnetic susceptibility over time (Fig. 6c) and the estimate of slurries viscosity through Marsh Funnel measurements (data not reported) show that the fluid properties were almost uniform during the whole injection, proving that the continuous recirculation was effective in preventing mZVI particle sedimentation during the injection and that the preparation setup was appropriate for a uniform dispersion of the particles.

3.5. mZVI distribution

The spatial distribution of the mZVI in the subsurface after injection was determined by magnetic susceptibility measurements performed on the core samples extracted in the proximity of the well according to the scheme reported in Fig. 1. The data set was post-processed in order to build a 3D reconstruction of the mZVI distribution. A near-neighbor algorithm was applied, and the conservation of iron mass was imposed to improve and constrain the results. Fig. 8 shows that a quite extended reactive zone within a ROI approximately equal to 0.8 m around the injection well was achieved, and the maximum measured distance reached by ZVI particles was 1.7 m. Particle migration was mainly horizontal from the well screen (located from 4.5 to 7 m), and mZVI was not detected above 4.5 m. All these findings suggest that, even if preferential flow paths were created (as evidenced by the pressure logs during delivery of the mZVI slurry), no migration pathways toward the upper layers nor daylighting, which are both typical of fracturing delivery in shallow aquifers, were evidenced (Velimirovic et al., 2014c).

The final distribution retrieved from core data analysis was predominantly determined by mZVI transport during injection, while a longer term mobility of the particles can be excluded: particles dispersed in the viscous guar gum slurry are stable for few hours, and when pumping was stopped they sedimented within a short time. Moreover, a re-mobilization after injection due to natural groundwater flow is very unlikely: when the pumping is stopped, the pore space around the injection well is filled by a highly viscous fluid, which will not be easily flushed out by groundwater flow. As a consequence, an almost stagnant region will be present in the injection area, until guar gum is not degraded (Krol et al., 2013).

Contrary to typical field injections of nZVI, where particles are mainly retained due to physical–chemical attractive interactions with the porous medium, and/or filtration of large particle aggregates (Johnson et al., 2013; Kocur et al., 2013; Krol et al., 2013; Messina and Marchisio, 2015; Tiraferri et al., 2011), in this field application the mZVI transport and retention were likely controlled mainly by straining. The final mZVI distribution is inhomogeneous along the vertical direction, and reflects the alternation of coarser layers (in the upper

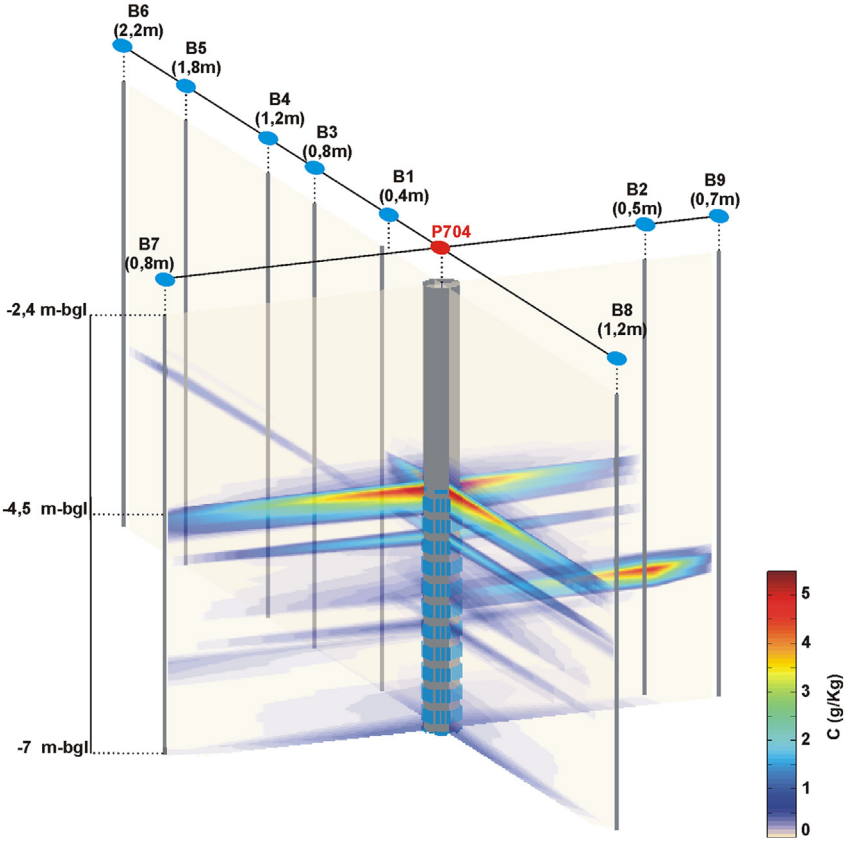

Fig. 8. mZVI distribution in the subsurface after injection reconstructed from magnetic susceptibility measurements on core logs.

Please cite this article as: Luna, M., et al., Pressure-controlled injection of guar gum stabilized microscale zerovalent iron for groundwater remediation, J. Contam. Hydrol. (2015), http://dx.doi.org/10.1016/j.jconhyd.2015.04.007

part, down to approximately 5 m from ground level) and finer layers (in the lower part, from 5 to 7 m). A limited mobility was observed in the lower layers, where the ratio of particle to sand grain diameter is above the straining threshold. The particles propagated mainly in the upper layer (4.5–5 m) where the ratio of particle size to aquifer grain size is close to the limit value for straining (Table 1). Here the highest mZVI concentration (5 g/kg in the core sample at 0.5 m distance from the well) and a more homogenous distribution were observed. Sedimentation within the porous medium during the injection is not likely to have played a significant role on the final iron distribution, since the mZVI slurry was designed in order to have a sedimentation half time longer than the duration of the injection. Also particle deposition controlled by DLVO physical-chemical interactions did not represent a major retention mechanism, since laboratory transport tests performed on similar materials (mZVI coated by guar gum and natural sand) evidenced an overall repulsion between particles and the porous medium (Dalla Vecchia et al., 2009b; Tosco et al., 2014a).

3.6. Groundwater monitoring

Since the focus of the pilot test was on the effective delivery of the mZVI in the subsurface, and the reactivity towards contaminants was considered of secondary importance, the installation of monitoring wells close to the injection point was avoided in order to minimize the risk of preferential flow path generation and product daylighting during the injection. For this reason the only available sampling point to evaluate the contaminant degradation is the injection well itself.

The monitoring of groundwater ORP and pH (shown in Fig. 9a) showed a significant decline in redox potential (from 102 mV to −220 mV), establishing highly reducing conditions, and a pH increase (from 5.6 to 8.2) one day after mZVI injection.

Both the decline in the redox potential and increase in pH values can be explained by the anaerobic corrosion of the injected mZVI (Gillham and Ohannesin, 1994). The polymer concentration measured in the injection well P704 one day after injection was 1.1 g/l, while 0.35 g/l was measured after 12 days. After 29 days, guar gum concentrations were below detection limits (50 mg/l) indicating fast guar gum biodegradation and/or removal by groundwater flow (Velimirovic et al., 2014b).

The results on the contaminant reduction obtained during the groundwater monitoring are shown in Fig. 9b. One day after injection, the removal efficiency of PCE, TCE and cDCE was 94%, 96% and 100%, respectively. The appearance of intermediate- and end-products of chlorinated hydrocarbons dehalogenation (namely chloroethane CA, vinyl chloride VC, ethene and ethane) proved that the observed decrease in CAHs concentration was not only due to dilution by the injected fluid. Indeed increased concentrations of CA, ethene and ethane after injection were measured and are explicable by reduction processes initiated by injected mZVI, while the presence of VC as an intermediate product can be explained by a partial hydrogenolysis pathway, which can be attributed to the impact of guar gum on iron reactivity (Velimirovic et al., 2012). The accumulation of cDCE observed 57 days after injection suggests that also biological processes may have been induced by mZVI injection, as a consequence of hydrogen gas production, pH increase, reducing conditions (Truex et al., 2011; Wei et al., 2010) and guar gum degradation. However, this aspect needs to be further investigated to prove the contribution of biological processes.

4. Conclusion

The present study aimed at developing and testing a design procedure and a pilot setup for the pressure-controlled injection of shear thinning slurries of iron particles for the remediation of contaminated sites. The method was applied and proved successful in a pilot injection of commercially available guar gum stabilized mZVI particles, despite the relatively low hydraulic conductivity of the aquifer system. The injection of the slurry was performed in a flow regime on the threshold between permeation and fracturing, generating a reactive zone of about 0.8 m around the injection well, with maximum migration distance of the mZVI particles of 1.7 m.

The use of mZVI rather than nZVI was preferred in this study due to the lower cost (1/20 to 1/3 compared to nZVI), lower

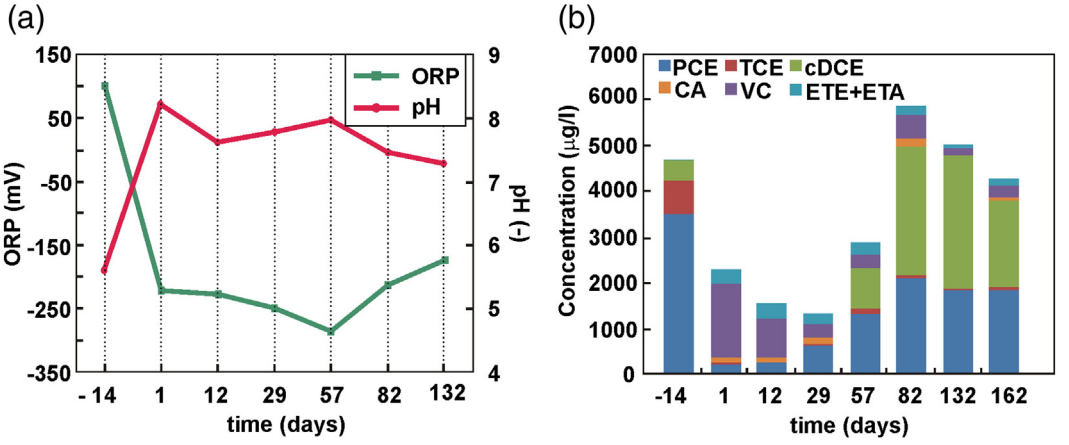

Fig. 9. Post-injection monitoring in P704 of (a) pH and ORP, and (b) concentration of tetrachloroethene (PCE), trichloroethene (TCE), cis-dichloroethene (cDCE), chloroethane (CA), vinylchloride (VC), ethene and ethane (ETE + ETA).

Please cite this article as: Luna, M., et al., Pressure-controlled injection of guar gum stabilized microscale zerovalent iron for groundwater remediation, J. Contam. Hydrol. (2015), http://dx.doi.org/10.1016/j.jconhyd.2015.04.007

corrosion rate (10 to 30 times lower than nZVI, (Velimirovic et al., 2014a)), and easier handling of microsized particles (provided as a dry powder). The design of this pilot test, and in general of any field-scale mZVI or nZVI delivery, is the result of the compromise among different, and often contrasting, needs: the slurry viscosity has to be sufficiently high to keep particles suspended until delivered into the porous medium, but sufficiently low to limit the injection pressure below or close to the critical pressure of the aquifer; the discharge rate is to be sufficiently low to limit the injection pressure, but sufficiently high to complete the delivery within the sedimentation time of the particles; the monitoring setup must allow a reliable, real-time control of all relevant parameters during injection (discharge rate, injected concentration, delivery pressure) and a cost-affordable but detailed reconstruction of the spatial distribution of the iron after injection, but must not interfere with the injection operations themselves. In this paper, a possible approach to mediate among these contrasting requirements was proposed. The coupled analysis of preliminary laboratory tests (sedimentation, reactivity and viscosity tests) and field characterization (step rate injection tests) was used to determine the optimal slurry composition, injection rate and injected volume. A complete setup for slurry preparation, injection and monitoring was designed and applied to optimize injection operations and monitoring by adopting low cost and fast solutions. We demonstrated that it is possible to prepare large volumes of mZVI slurry, hydrating the guar gum at ambient temperature with a high shear processor in order to speed up the preparation and to minimize the presence of undissolved biopolymer. An injection well was specifically designed to prevent daylighting of the product after the determination of the range of sustainable discharge rate and of the critical pressure. A monitoring setup for in-line control of several parameters (pressure injection and water level at the well, magnetic susceptibility of the injected fluid, discharge rate, slurry viscosity) during the injection via simple and fast measuring techniques allowed to understand and to control the phenomena occurring in the subsurface in real time. In particular, magnetic susceptibility measurements, conducted with a commercially available and low-cost sensor, were able to provide information on the stability and the mZVI concentration of the injected fluid, and to easily detect the presence of the iron in the soil cores retrieved from the subsurface, with an accuracy comparable to results obtained via chemical analysis and remarkably reduced costs.

The authors believe that, even if the design protocol and the experimental setup presented in this work were specifically intended for mZVI, they can also be easily adapted to the delivery of nZVI, and of any viscous reactant for groundwater remediation, since the guiding principles are similar, and design constraints, procedures and field equipment are of general validity.

Acknowledgments

Part of the work was financed by the EU research project AQUAREHAB (FP7—G. A. Nr. 226565).

Appendix A. Supplementary data

Supplementary data to this article can be found online at http://dx.doi.org/10.1016/j.jconhyd.2015.04.007.

References

Bennett, P., He, F., Zhao, D., Aiken, B., Feldman, L., 2010. In situ testing of metallic iron nanoparticle mobility and reactivity in a shallow granular aquifer. J. Contam. Hydrol. 116 (1-4), 35–46.

Bradford, S.A., Simunek, J., Bettahar, M., van Genuchten, M.T., Yates, S.R., 2006. Significance of straining in colloid deposition: evidence and implications. Water Resour. Res. 42 (12), W12S15.

Cameselle, C., Reddy, K., Darko-Kagya, K., Khodadoust, A., 2013. Effect of dispersant on transport of nanoscale iron particles in soils: zeta potential measurements and column experiments. J. Environ. Eng. 139 (1), 23–33.

Cantrell, K.J., Kaplan, D.I., Gilmore, T.J., 1997. Injection of colloidal Fe0 particles in sand with shear-thinning fluids. J. Environ. Eng. 123 (8), 786–791.

Comba, Sethi, R., 2009. Stabilization of highly concentrated suspensions of iron nanoparticles using shear-thinning gels of xanthan gum. Water Research 43 (15), 3717–3726.

Comba, S., Dalmazzo, D., Santagata, E., Sethi, R., 2011. Rheological characterization of xanthan suspensions of nanoscale iron for injection in porous media. J. Hazard. Mater. 185 (2–3), 598–605.

Cook, S.M., 2009. Assessing the Use and Application of Zero-Valent Iron Nanoparticle Technology for Remediation at Contaminated Sites. U.S. Environmental Protection Agency.

Dalla Vecchia, E., Coisson, M., Appino, C., Vinai, F., Sethi, R., 2009a. Magnetic characterization and interaction modeling of zerovalent iron nanoparticles for the remediation of contaminated aquifers. J. Nanosci. Nanotechnol. 9 (5), 3210–3218.

Dalla Vecchia, E., Luna, M., Sethi, R., 2009b. Transport in porous media of highly concentrated iron micro- and nanoparticles in the presence of xanthan gum. Environ. Sci. Technol. 43 (23), 8942–8947.

Di Molfetta, A., Sethi, R., 2006. Clamshell excavation of a permeable reactive barrier. Environ. Geol. 50 (3), 361–369. http://dx.doi.org/10.1007/s00254-006-0215-3.

Di Molfetta, A., Sethi, R., 2012. Ingegneria degli acquiferi. Springer.

DuBois, M., Gilles, K.A., Hamilton, J.K., Rebers, P.A., Smith, F., 1956. Colorimetric method for determination of sugars and related substances. Anal. Chem. 28 (3), 350–356.

Elimelech, M., O'Melia, C.R., 1990. Kinetics of deposition of colloidal particles in porous media. Environ. Sci. Technol. 24 (10), 1528–1536.

Elliott, D.W., Zhang, W.X., 2003. Field assessment of nanoscale bimetallic particles for groundwater treatment. Abstr. Pap. Am. Chem. Soc. 225, U971-U971.

EPA, U.S., 2003. Cost and Performance Summary Report In Situ Chemical Reduction at the Marshall Space Flight Center, Source Area 2. Huntsville, Alabama.

Flores Orozco, A., Velimirovic, M., Tosco, T., Kemna, A., Sapion, H., Klaas, N., Sethi, R., Bastiaens, L., 2015. Monitoring the Injection of Microscale Zerovalent Iron Particles for Groundwater Remediation by Means of Complex Electrical Conductivity Imaging. Environmental Science & Technology 49 (9), 5593–5600.

Freyria, F.S., Bonelli, B., Sethi, R., Armandi, M., Belluso, E., Garrone, E., 2011. Reactions of acid orange 7 with iron nanoparticles in aqueous solutions. J. Phys. Chem. C 115 (49), 24143–24152.

Gastone, F., Tosco, T., Sethi, R., 2014a. Green stabilization of microscale iron particles using guar gum: bulk rheology, sedimentation rate and enzymatic degradation. J. Colloid Interface Sci. 421, 33–43.

Gastone, F., Tosco, T., Sethi, R., 2014b. Guar gum solutions for improved delivery of iron particles in porous media (part 1): porous medium rheology and guar gum-induced clogging. J. Contam. Hydrol. 166, 23–33.

Gillham, R.W., Ohannesin, S.F., 1994. Enhanced degradation of halogenated aliphatics by zero valent iron. Ground Water 32 (6), 958–967.

Hazen, A., 1892. Some physical properties of sands and gravels, with special reference to their use in filtration. 4th Annual Report, Massachusetts State Board of Health, Pub. Doc. 34, pp. 539–556.

Hazen, A., 1911. Discussion of dams on sand foundations. Trans. Am. Soc. Civ. Eng. 73, 199–203.

He, F., Zhao, D., 2005. Preparation and characterization of a new class of starch-stabilized bimetallic nanoparticles for degradation of chlorinated hydrocarbons in water. Environ. Sci. Technol. 39 (9), 3314–3320.

He, F., Zhao, D., Paul, C., 2010. Field assessment of carboxymethyl cellulose stabilized iron nanoparticles for in situ destruction of chlorinated solvents in source zones. Water Res. 44 (7), 2360–2370.

Hosseini, S.M., Tosco, T., 2013. Transport and retention of high concentrated nano-Fe/Cu particles through highly flow-rated packed sand column. Water Res. 47 (1), 326–338.

Hosseini, S.M., Ataie-Ashtiani, B., Kholghi, M., 2011. Nitrate reduction by nano-Fe/Cu particles in packed column. Desalination 276 (1–3), 214–221.

Hydutsky, B.W., Mack, E.J., Beckerman, B.B., Skluzacek, J.M., Mallouk, T.E., 2007. Optimization of nano- and microiron transport through sand columns using polyelectrolyte mixtures. Environ. Sci. Technol. 41 (18).

Please cite this article as: Luna, M., et al., Pressure-controlled injection of guar gum stabilized microscale zerovalent iron for groundwater remediation, J. Contam. Hydrol. (2015), http://dx.doi.org/10.1016/j.jconhyd.2015.04.007

Johnson, R.L., Nurmi, J.T., O'Brien Johnson, G.S., Fan, D., O'Brien Johnson, R.L., Shi, Z., Salter-Blanc, A.J., Tratnyek, P.G., Lowry, G.V., 2013. Field-scale transport and transformation of carboxymethylcellulose-stabilized nano zero-valent iron. Environ. Sci. Technol. 47 (3), 1573–1580.

Kanel, S.R., Manning, B., Charlet, L., Choi, H., 2005. Removal of arsenic(III) from groundwater by nanoscale zero-valent iron. Environ. Sci. Technol. 39 (5), 1291–1298.

Kirschling, T.L., Golas, P.L., Unrine, J.M., Matyjaszewski, K., Gregory, K.B., Lowry, G.V., Tilton, R.D., 2011. Microbial bioavailability of covalently bound polymer coatings on model engineered nanomaterials. Environ. Sci. Technol. 45 (12), 5253–5259.

Kocur, C.M., O'Carroll, D.M., Sleep, B.E., 2013. Impact of nZVI stability on mobility in porous media. J. Contam. Hydrol. 145, 17–25.

Krol, M.M., Oleniuk, A.J., Kocur, C.M., Sleep, B.E., Bennett, P., Zhong, X., O'Carroll, D.M., 2013. A field-validated model for in situ transport of polymer-stabilized nZVI and implications for subsurface injection. Environ. Sci. Technol. 47 (13), 7332–7340.

Liu, Y.Q., Choi, H., Dionysiou, D., Lowry, G.V., 2005. Trichloroethene hydrodechlorination in water by highly disordered monometallic nanoiron. Chem. Mater. 17 (21), 5315–5322.

Luna, M., Gastone, F., Tosco, T., Sethi, R., Velimirovic, M., Bastiaens, L., Gemoets, J., Muyshond, R., Sapion, H., Klaas, N., 2013. Low pressure injection of guar gum stabilized microscale zerovalent iron particles: a pilot study. In: Bastiaens, L. (Ed.), Water Technology and Management Symposium VITO. Leuven, Belgium, pp. 78–83.

Macé, C., Desrocher, S., Gheorghiu, F., Kane, A., Pupeza, M., Cernik, M., Kvapil, P., Venkatakrishnan, R., Zhang,, W.-x., 2006. Nanotechnology and groundwater remediation: a step forward in technology understanding. Remediat. J. 16 (2), 23–33.

Messina, F., Marchisio, D.L., Sethi, R., 2015. An extended and total flux normalized correlation equation for predicting single-collector efficiency. Journal of Colloid and Interface Science 446, 185–193.

Mitchell, J.K., Soga, K., 2005. Fundamentals of Soil Behavior. John Wiley and Sons Inc.

Moraci, N., Calabrò, P.S., 2010. Heavy metals removal and hydraulic performance in zero-valent iron/pumice permeable reactive barriers. J. Environ. Manag. 91 (11), 2336–2341.

Mueller, N.C., Braun, J., Bruns, J., Černík, M., Rissing, P., Rickerby, D., Nowack, B., 2012. Application of nanoscale zero valent iron (NZVI) for groundwater remediation in Europe. Environ. Sci. Pollut. Res. 19 (2), 550–558.

Nurmi, J.T., Tratnyek, P.G., Sarathy, V., Baer, D.R., Amonette, J.E., Pecher, K., Wang, C.M., Linehan, J.C., Matson, D.W., Penn, R.L., Driessen, M.D., 2005. Characterization and properties of metallic iron nanoparticles: spectroscopy, electrochemistry, and kinetics. Environ. Sci. Technol. 39 (5), 1221–1230.

O'Carroll, D., Sleep, B., Krol, M., Boparai, H., Kocur, C., 2013. Nanoscale zero valent iron and bimetallic particles for contaminated site remediation. Adv. Water Resour. 51, 104–122.

Phenrat, T., Saleh, N., Sirk, K., Tilton, R.D., Lowry, G.V., 2007. Aggregation and sedimentation of aqueous nanoscale zerovalent iron dispersions. Environ. Sci. Technol. 41 (1), 284–290.

Phenrat, T., Saleh, N., Sirk, K., Kim, H.J., Tilton, R.D., Lowry, G.V., 2008. Stabilization of aqueous nanoscale zerovalent iron dispersions by anionic polyelectrolytes: adsorbed anionic polyelectrolyte layer properties and their effect on aggregation and sedimentation. J. Nanoparticle Res. 10 (5), 795–814.

Phenrat, T., Cihan, A., Kim, H.-J., Mital, M., Illangasekare, T., Lowry, G.V., 2010. Transport and deposition of polymer-modified Fe0 nanoparticles in 2-D heterogeneous porous media: effects of particle concentration, Fe0 content, and coatings. Environ. Sci. Technol. 44 (23), 9086–9093.

Quinn, J., Geiger, C., Clausen, C., Brooks, K., Coon, C., O'Hara, S., Krug, T., Major, D., Yoon, W.S., Gavaskar, A., Holdsworth, T., 2005. Field demonstration of DNAPL dehalogenation using emulsified zero-valent iron. Environ. Sci. Technol. 39 (5), 1309–1318.

Raychoudhury, T., Tufenkji, N., Ghoshal, S., 2014. Straining of polyelectrolyte-stabilized nanoscale zero valent iron particles during transport through granular porous media. Water Res. 50, 80–89.

Reddy, K.R., Khodadoust, A.P., Darko-Kagya, K., 2011. Transport and reactivity of lactate-modified nanoscale iron particles in PCP-contaminated soils. J. Hazard. Toxic Radioact. Waste Manage. 16 (1), 68–74.

Rorabaugh, M.I., 1953. Graphical and theoretical analysis of step-drawdown test of artesian wells. Proc. Am. Soc. Civ. Eng. 79 (362), 1–23.

Saleh, N., Sirk, K., Liu, Y., Phenrat, T., Dufour, B., Matyjaszewski, K., Tilton, R.D., Lowry, G.V., 2007. Surface modifications enhance nanoiron transport and NAPL targeting in saturated porous media. Environ. Eng. Sci. 24 (1), 45–57.

Schlicker, O., Ebert, M., Fruth, M., Weidner, M., Wüst, W., Dahmke, A., 2000. Degradation of TCE with iron: the role of competing chromate and nitrate reduction. Ground Water 38 (3), 403–409.

Schrick, B., Hydutsky, B.W., Blough, J.L., Mallouk, T.E., 2004. Delivery vehicles for zerovalent metal nanoparticles in soil and groundwater. Chem. Mater. 16 (11), 2187–2193.

Sethi, R., 2011. A dual-well step drawdown method for the estimation of linear and non-linear flow parameters and wellbore skin factor in confined aquifer systems. J. Hydrol. 400 (1-2), 187–194.

Sorbie, K.S., Clifford, P.J., Jones, E.R.W., 1989. The rheology of pseaudoplastic fluids in porous media using network modeling. J. Colloid Interface Sci. 130 (2), 508–534.

Su, C., Puls, R.W., 2004. Nitrate reduction by zerovalent iron: effects of formate, oxalate, citrate, chloride, sulfate, borate, and phosphate. Environ. Sci. Technol. 38 (9), 2715–2720.

Su, C., Puls, R.W., Krug, T.A., Watling, M.T., O'Hara, S.K., Quinn, J.W., Ruiz, N.E., 2012. A two and half-year-performance evaluation of a field test on treatment of source zone tetrachloroethene and its chlorinated daughter products using emulsified zero valent iron nanoparticles. Water Res. 46 (16), 5071–5084.

Tiraferri, A., Sethi, R., 2009. Enhanced transport of zerovalent iron nanoparticles in saturated porous media by guar gum. J. Nanoparticle Res. 11 (3), 635–645.

Tiraferri, A., Chen, K.L., Sethi, R., Elimelech, M., 2008. Reduced aggregation and sedimentation of zero-valent iron nanoparticles in the presence of guar gum. J. Colloid Interface Sci. 324 (1-2), 71–79.

Tiraferri, A., Tosco, T., Sethi, R., 2011. Transport and retention of microparticles in packed sand columns at low and intermediate ionic strengths: Experiments and mathematical modeling. Environmental Earth Sciences 63 (4), 847–859.

Tosco, T., Sethi, R., 2010. Transport of non-newtonian suspensions of highly concentrated micro- and nanoscale iron particles in porous media: a modeling approach. Environ. Sci. Technol. 44 (23), 9062–9068.

Tosco, T., Gastone, F., Sethi, R., 2014a. Guar gum solutions for improved delivery of iron particles in porous media (part 2): iron transport tests and modeling in radial geometry. J. Contam. Hydrol. 166, 34–51.

Tosco, T., Petrangeli Papini, M., Cruz Viggi, C., Sethi, R., 2014b. Nanoscale iron particles for groundwater remediation: a review. J. Clean. Prod. 77, 10–21.

Truex, M.J., Vermeul, V.R., Mendoza, D.P., Fritz, B.G., Mackley, R.D., Oostrom, M., Wietsma, T.W., Macbeth, T.W., 2011. Injection of zero-valent iron into an unconfined aquifer using shear-thinning fluids. Ground Water Monit. Rem. 31 (1), 50–58.

USEPA, 1998. Soil Sampling Technology Geoprobe Systems, Inc. LargeBore Soil Sampler. Environmental Technology Verification Report. DIANE Publishing.

Velimirovic, M., Chen, H., Simons, Q., Bastiaens, L., 2012. Reactivity recovery of guar gum coupled mZVI by means of enzymatic breakdown and rinsing. J. Contam. Hydrol. 142–143, 1–10.

Velimirovic, M., Larsson, P.-O., Simons, Q., Bastiaens, L., 2013. Reactivity screening of microscale zerovalent irons and iron sulfides towards different CAHs under standardized experimental conditions. J. Hazard. Mater. 252–253, 204–212.

Velimirovic, M., Carniato, L., Simons, Q., Schoups, G., Seuntjens, P., Bastiaens, L., 2014a. Corrosion rate estimations of microscale zerovalent iron particles via direct hydrogen production measurements. J. Hazard. Mater. 270, 18–26.

Velimirovic, M., Simons, Q., Bastiaens, L., 2014b. Guar gum coupled microscale ZVI for in situ treatment of CAHs: continuous-flow column study. J. Hazard. Mater. 265, 20–29.

Velimirovic, M., Tosco, T., Uyttebroek, M., Luna, M., Gastone, F., De Boer, C., Klaas, N., Sapion, H., Eisenmann, H., Larsson, P.-O., Braun, J., Sethi, R., Bastiaens, L., 2014c. Field assessment of guar gum stabilized microscale zerovalent iron particles for in-situ remediation of 1,1,1-trichloroethane. J. Contam. Hydrol. 164, 88–99.

Wang, Q., Ellis, P.R., Ross-Murphy, S.B., 2008. Dissolution kinetics of water-soluble polymers: the guar gum paradigm. Carbohydr. Polym. 74 (3), 519–526.

Wei, Y.-T., Wu, S.-C., Chou, C.-M., Che, C.-H., Tsai, S.-M., Lien, H.-L., 2010. Influence of nanoscale zero-valent iron on geochemical properties of groundwater and vinyl chloride degradation: a field case study. Water Res. 44 (1), 131–140.

Westerhoff, P., 2003. Reduction of nitrate, bromate, and chlorate by zero valent iron (Fe0). J. Environ. Eng. 129 (1), 10–16.

Xu, S.P., Gao, B., Saiers, J.E., 2006. Straining of colloidal particles in saturated porous media. Water Resour. Res. 42 (12). http://dx.doi.org/10.1029/2006wr004948.

Xue, D., Sethi, R., 2012. Viscoelastic gels of guar and xanthan gum mixtures provide long-term stabilization of iron micro- and nanoparticles. J. Nanoparticle Res. 14 (11) (Art. No.: 1239).

Zhang, W.X., 2003. Nanoscale iron particles for environmental remediation: an overview. J. Nanoparticle Res. 5 (3-4), 323–332.

Zolla, V., Freyria, F.S., Sethi, R., Di Molfetta, A., 2009. Hydrogeochemical and biological processes affecting the long-term performance of an iron-based permeable reactive barrier. J. Environ. Qual. 38 (3), 897–908.

Please cite this article as: Luna, M., et al., Pressure-controlled injection of guar gum stabilized microscale zerovalent iron for groundwater remediation, J. Contam. Hydrol. (2015), http://dx.doi.org/10.1016/j.jconhyd.2015.04.007